https://doi.org/10.5194/egusphere-2024-845
Preprint. Discussion started: 24 April 2024

Sedimentary organic matter signature hints at the phytoplankton-driven Biological Carbon Pump in the Central Arabian Sea

Medhavi Pandey[1,2], Haimanti Biswas[1,2*], Daniel Birgel[3], Nicole Burdanowitz[3], Birgit Gaye[3]

[1]CSIR National Institute of Oceanography, Biological Oceanography Division, Dona Paula, Goa 403004. India.
[2]Academy of Scientific and Innovative Research (AcSIR), Ghaziabad-201002, India.
[3]Institute for Geology, Center for Earth System Research and Sustainability (CEN), Universität Hamburg, Bundesstraße55, 20146, Hamburg, Germany.
*Corresponding Author's email: haimanti.biswas.nio@gmail.com; haimanti.biswas@nio.org

Abstract

The Central Arabian Sea, a unique tropical basin is profoundly impacted by monsoon wind reversal affecting its surface circulation and biogeochemistry. Phytoplankton bloom associated with high biological productivity and particle flux occurs in the northern part of the central Arabian Sea due to summer monsoon-induced open ocean upwelling and winter convection. The core Oxygen Minimum Zone (OMZ) at the intermediate water depths is another important feature of the north-central Arabian Sea and fades southward. In this study, we have attempted to interlink how these factors collectively impact phytodetrital export to the sediment. Short sediment core top (1cm) samples representing the recent particle flux signatures were analyzed from 5 locations (21° to 11° N; 64° E) in the central Arabian Sea. The C_{37} alkenone-based sea surface temperature (SST) proxy indicated cooler SST (27.6 ± 0.25 °C) in the north mostly due to upwelling (summer) and convective mixing (winter) and warmer (0.4 °C) in the south, which usually remains nutrient-poor. This trend was consistent with the satellite-derived average SST values (2017–2020). Lipid biomarker analysis suggested that dinoflagellates were the highest contributor as indicated in dinosterol and its degradative product dinostanol followed by brassicasterol, and C_{37} alkenone representing diatoms, and coccolithophores, respectively. The stations in the north (21–15° N) that largely experience periodic phytoplankton blooms and is influenced by the thick OMZ revealed the highest contents of organic matter, diatom frustules (diversity and abundance) dominated by large thickly silicified cells (e.g. *Coscinodiscus* and *Rhizosolenia*), and phytoplankton organic biomarkers, but lower zooplankton biomarkers (cholesterol and cholestanol). Whereas relatively smaller chain-forming centric (e.g. *Thalassiosira*) and pennate (e.g. *Pseudo-nitzschia*, *Nitzschia, Thalassionema*) diatom frustules along with lower phytoplankton biomarker contents were found in the south where zooplankton biomarkers and silicious radiolarians were more abundant. The probable impacts of the presence of the OMZ along the sampling transect on particle flux related to the phytoplankton community, zooplankton grazing along with other factors have also been discussed.

Keywords: Phytodetritus; North Indian Ocean; Monsoon; Biomarkers; Brassicasterol; Dinosterol

https://doi.org/10.5194/egusphere-2024-845
Preprint. Discussion started: 24 April 2024

Introduction

Marine phytoplankton modulate the global carbon cycle by fixing almost 48 Gt C annually (Singh and Ahluwalia, 2013) which corresponds to 50% of global primary production (Field et al., 1998; Behrenfeld et al., 2006). This amount of organic matter produced within the euphotic layers, where 1% of solar light arrives, supports the entire marine food chain including the benthic population. Nearly 10% of this organic matter (large and dense phytodetritus) sinks to the upper mesopelagic ocean and gets further fragmented by zooplankton and microbially remineralized on its descent into the deep ocean. Only 1–3% of this phytodetritus can reach the seafloor below 1000 m depth (Iversen, 2023) and can be stored for hundreds to millions of years (Buesseler, 1998) and is called sequestration flux. This way of trapping carbon from the atmosphere to the ocean interior mediated by phytoplankton is called the Biological Carbon Pump (BCP) (Volk and Hoffert, 1985; Le Moigne, 2019; Iversen, 2023 and references therein). However, the organic matter in the surface sediment can be further modified biogeochemically. The strength of BCP is governed by many factors, such as heterotrophic remineralization of organic matter, dissolved oxygen (DO) levels, temperature, phytoplankton community composition, cell size, and zooplankton activity (Marsay et al., 2015; Keil et al., 2016; Cavan et al., 2017; Engel et al., 2017; Iversen, 2023). Out of multiple factors controlling the efficacy of the BCP, phytoplankton community composition (that controls organic matter stoichiometry), zooplankton grazing (Cavan et al., 2017), and the presence of well-oxygenated water (Keil et al., 2016) are crucial. Thus, understanding the functioning of the marine BCP in productive marine ecosystems needs attention, particularly in the context of changing climate (Iversen, 2023).

Marine organic matter preserved in sediments in the forms of diatom frustules, dinoflagellate cysts, and organic biomarkers (sterols, alkenones) could be potential proxies for understanding organic matter transport from the surface to the deep sea floor (Liu et al., 2013; Hu et al., 2020; Xiong et al., 2020 and references therein). The responses of phytoplankton to changing climate as well as other environmental variables can be retrieved from the sediments and may help predict future primary production, community shifts in marine ecosystems, and the ocean's role as a carbon sink. The siliceous frustules of diatoms can be more resistant to grazing and degradation and can be better preserved in sediments. Sedimentary organic carbon, nitrogen, and their ratios, diatom frustules, and organic biomarkers (e.g. sterols and alkenones) are used to reconstruct past phytoplankton community shift and temperature (Schubert et al., 1998; Liu et al., 2013; Rodríguez-Miret et al., 2023). The lipid biomarkers of phytodetritus from the surface sediments can also provide valuable information about the surface processes controlling phytoplankton growth and their transport to the sediment (Xiong et al., 2020). For example in a study by Peng et al. (2023), phytoplankton community shift was evident in lipid biomarkers in the sediment core samples from the East China Sea. In a few studies, major phytoplankton lipid biomarkers like dinosterol, brassicasterol, and alkenone were also used to correlate their contents with palaeoproductivity and associated changes of the sea ice levels in the Arctic Ocean (Müller et al., 2011 and references therein).

The Arabian Sea, the northwestern part of the Indian Ocean, is a unique marine province with several characteristic features, for instance, the direct influence of monsoon winds on oceanographic and biogeochemical processes, high productivity (McCreary et al., 2009), and one of the thickest (200–1200 m) oxygen minimum zones (OMZ) in modern oceans (Banse et al., 2014). The entire area experiences periodic reversals of monsoon winds and in its surface circulation. During the summer (SW) monsoon, a low-level atmospheric Jet (the Findlater Jet; Findlater, 1971) blows parallel to the Omani and Somalia coasts, generating coastal and open

https://doi.org/10.5194/egusphere-2024-845
Preprint. Discussion started: 24 April 2024

ocean upwelling in its northern part. Subsequently, due to natural nutrient enrichment, phytoplankton blooms develop (Banse, 1987; Bhattathiri et al., 1996; Prasanna Kumar et al., 2000). In the winter (NE) monsoon, winds and surface circulation reverse and in the northern Arabian Sea the cooling and densification of surface water leads to convective mixing (Prasannakumar et al., 2001) that also fuels high phytoplankton growth (Madhupratap et al., 1996).

In the Arabian Sea, the magnitude of particle transfer to the deep sea floor is directly controlled by the surface processes (Schulte et al., 1999, Rixen et al., 2019a). The central Arabian Sea exhibits one of the highest particle flux rates (1.3–3.3 g C m^{-2} $year^{-1}$) (Haake et al., 1993) compared with other low-latitude seas (Rixen et al., 2019b). This is mostly associated with enhanced biological productivity governed by summer monsoon-induced upwelling and winter convection (Nair et al., 1989; Haake et al., 1993; Rixen et al., 2019a). Nevertheless, particle flux could vary significantly (Nair et al., 1989; Prahl et al., 2000) during the intermonsoon and premonsoon due to prevailing oligotrophy (Prasanna Kumar and Narvekar, 2005).

The impacts of atmospheric forcings and consequent biological response in the central Arabian Sea have been studied thoroughly during the joint Global Ocean Flux Studies (JGOFS, from 1987 to 2003). It was evident that the monsoon wind is the major controlling forcing of physical, chemical, and biological processes in the surface ocean (McCeary et al., 2009) with high spatial and seasonal variability (Prasanna Kumar and Narvekar, 2005). However, there was no further investigation in the last two decades, although ocean warming continued with high spatial variability (Roxy et al., 2016; Sharma et al., 2023 and references therein). Our previous study showed that diatom frustules retrieved from the surface sediments from the central (Pandey et al., 2023) and the eastern (Pandey and Biswas, 2023) Arabian Sea could be an efficient indicator of surface processes controlling euphotic phytoplankton communities. There are a few studies from the Arabian Sea characterizing sedimentary organic carbon using phytoplankton biomarkers (Schubert et al., 1998; Prahl et al., 2000; Schulte et al., 1999; 2000) suggesting such proxies from the surface sediment may be quite useful to understand the spatial variability in organic matter transport. Prahl et al. (2000) used phytoplankton biomarkers from sediment trap samples as well as from the surface sediments over a year from the central Arabian Sea (15°59′N, 61°30′E) and showed the seasonal variability in surface water conditions that modified biological productivity. Nevertheless, the degradation of organic matter in the water column could be quite high during their descent through the water column pointed out by Wakeham et al. (2002) in their work on lipids from the water column of the western Arabian Sea.

Importantly, the Arabian Sea is warming at a faster pace compared to other oceanic regions (Roxy et al., 2016; Sharma et al., 2023), and how the phytoplankton-driven organic matter transport may respond to that change is still poorly understood. Furthermore, recent modeling studies hinted at the possibility of thinning of the OMZ in the Arabian Sea that may substantially impact organic matter degradation within the water column, specifically in the southern part (Roxy et al., 2016). To fill this gap, in the present study, we ~~want to~~ address three major questions 1) Which phytoplankton group dominates the sedimentary organic matter in the various stations of the transect from north to south? 2) Does high spatial variability in the phytoplankton community composition driven by physical forcing also impact organic matter transport? 3) What are the possible factors (hydrography, physicochemical conditions, and atmospheric forcings) ~~being~~ responsible for such spatial variability in organic matter transport in this region? To address these questions, we have measured key parameters from surface

https://doi.org/10.5194/egusphere-2024-845
Preprint. Discussion started: 24 April 2024

sediments including lipid biomarkers, alkenone-based SST ~~reconstruction,~~ and diatom frustules combined with our recent observations on hydrography, biogeochemistry, and phytoplankton community (Silori et al., 2021; 2022; Chowdhury et al., 2021; Pandey et al., 2023).

2 Methodology

2.1. Sample collection

During cruise SSD–068 (Dec 2019 to Jan 2020) with *RV. Sindhu Sadhana* five short sediment cores were obtained using a multicorer (Ocean Scientific International Limited Maxi Multi-corer; core tubes 60 cm, outer diameter 11 cm and 10 cm inner diameter) along a transect from 11–21° N at 64° E (Fig. 1a). The~~se~~ short cores were collected at 21, 19, 15, 13, and 11° N with varying water depths between 3000–4500 m (Fig. 1a). The cores were subsampled onboard immediately at every 0.5 cm and ~~were~~ kept in pre-cleaned plastic containers at 0–4 °C. The advantages using multicorer is the better preservation of the topmost parts of the sediment core compared to other devices like box or gravity coring (Barnett et al., 1984). For this study we used the top 1 cm (0.5, 1) of the core for all related analyses.

2.2. Analytical method

2.2.1. Total inorganic carbon (TIC), total organic carbon (TOC), and total nitrogen (TN) contents

Sediment samples were dried at 60 °C overnight and ground using agate mortar and pestle. Aliquots (10 mg) of sediment samples were taken in tin capsules. Total carbon (TC) and TN were measured using a CHN Elemental analyzer (Euro Vector EA3000 series analyzer) at the Central Analytical Facility of CSIR-National Institute of Oceanography, Goa, India) against soil reference material used for carbon and nitrogen (Thermofisher Scientific, Cambridge, UK) with an analytical error of < 2%. The TIC contents were measured against the calcium carbonate ($CaCO_3$) standard (Merck, Germany) in a coulometer attached to an acidification module (Model CM5015 (UIC, USA). The accuracy and precision obtained from the results were within ± 1.25%. TOC values were calculated by the difference between TC and TIC (TOC =TC-TIC).

2.2.2. Analysis of silica-bearing organisms from sediments

The diatom frustules and other siliceous organisms from sediments were enumerated following the method by Armbrecht et al.~~,~~ (2018). The dried sediment subsamples (50 mg) were taken in a 50 mL sterile polypropylene tube and ~~were~~ treated ~~chemically~~ with 10% HCl, 30% H_2O_2, and 0.01 N anhydrous sodium diphosphate ($Na_4P_2O_7$) for removing carbonate, organic matter, and fine clay, respectively. After each chemical treatment, samples were washed thrice with Milli-Q water. Finally, the residue remaining after the last rinse and decantation was diluted with Milli-Q to 10 mL and was homogenized. A small portion (1 mL) from this homogenized solution was analyzed under an inverted microscope (Nikon Ti2) in a Sedgewick rafter counting chamber (Pyser, UK) at 400–600× magnification. The classical identification keys by Tomas (1997), Desikachary (1989) and http://www.algaebase.org were used. No centrifugation was used in this process to restrict the breaking of frustules. Further, the diatoms more than half in size were considered complete valves (Abrantes and Sancetta, 1985). The diatom abundance was expressed as valves g^{-1} dry sediment. Radiolarians were also enumerated along with diatom frustules and ~~were represented~~ as individuals g^{-1}.

https://doi.org/10.5194/egusphere-2024-845
Preprint. Discussion started: 24 April 2024

2.2.3 Biomarker analysis and temperature proxy

Lipid biomarker analyses were carried out at the Institute for Geology, University of Hamburg, Germany. About 11 to 19 g of freeze-dried and ground samples were used to obtain total lipid extracts (TLEs) by using an Accelerated Solvent Extractor (ASE200, DIONEX). Before extraction, ~~a known amount (~~10 ng μL^{-1}~~)~~ of internal standards (14-heptacosanone, nonadecanol, and dialkylglycerol ether-18 (DAGE-18)) were added to the samples. The ASE extraction for each sample was carried out at 100°C and 1000 PSI for 5 minutes in 3 cycles by using the solvent mixture dichloromethane: methanol (DCM: MeOH, 9:1). The TLEs were then concentrated with rotary evaporation and ~~were~~ separated later into a hexane-soluble (adding *n*-hexane) and hexane-insoluble (adding DCM) fraction via $NaSO_4$ column chromatography. To separate the hexane-soluble fraction into a neutral- and acid fraction via saponification (at 85°C for 2 hrs) a 5 % potassium hydroxide (KOH) in MeOH solution was added to this fraction. Then, the neutral fractions were obtained by adding n-hexane to the saponified fraction, vortexing, and pipetting the neutral fraction containing *n*-hexane layer into a new vial. The neutral fractions were then separated into apolar-, ketone- (containing alkenones), and polar fractions (containing sterols, stanols) by column chromatography packed with deactivated silica gel (5 % H_2O, 60 µm mesh) using the solvents n-hexane, DCM, and DCM:MeOH (1:1), respectively. We took 50% splits of the ketone- and polar fractions and put them together, as some of the sterols and added standards for the sterol fraction were found in the ketone fraction, too. For the derivatization of these fractions, a mixture of 200 µL BSTFA: Pyridin (1:1) was added to the dried sample and heated at 80°C for 2 hrs followed by drying under an N_2 environment.

To quantify the alkenones and sterols the samples were measured with a Thermo Scientific Trace 1310 gas chromatography coupled to a flame ionization detector (GC-FID) equipped with a Thermo Scientific TG-5MS column (30 m, 0.25 mm, 0.25 µm). H_2 as carrier gas was used with a flow rate of 35 mL $minute^{-1}$ and the PTV injector started at 50°C ramped with 10°C/s to 325°C in a splitless mode. For the alkenones, the initial GC temperature was programmed to 50°C (held 1 minute) and then ramped to a temperature of 230 °C with an increased rate of 20 °C $minute^{-1}$, then increased ~~with~~ 4.5°C $minute^{-1}$ to 260 °C and finally increased ~~the temperature with~~ 6 °C $minute^{-1}$ to 325 °C which was held for 15 minutes. The peaks of alkenones were identified by comparing the retention time for peaks of the samples with a known working sediment standard. Quantification of the alkenones was done by using 14-heptacosane and tetratriacontane with a known amount (10 ng μL^{-1}) as external standards. Repeated measurements of the external standards yielded a quantification precision of 13 % (14-heptacosanone) and 8 % (tetratriacontane). The alkenone saturation index was calculated using the equation by Prahl et al. (1988):

$$U_{37}^{k\prime} = \frac{C_{37:2}}{C_{37:2} + C_{37:3}}$$

to convert the $U_{37}^{k\prime}$ index to SSTs we have used the core top calibration of Indian Ocean sediments (Sonzogni et al., 1997):

$$SST = \frac{U_{37}^{k\prime} - 0.043}{0.033}$$

For each sample, at least a duplicate measurement was conducted, which yielded an average precision of 0.1°C (1SD). Replicate extractions of a working standard sediment (n=2) and its duplicate measurements of each replicate yielded to an average precision of 0.5°C (1 SD).

https://doi.org/10.5194/egusphere-2024-845
Preprint. Discussion started: 24 April 2024

For the quantification of the sterols, the initial GC temperature was 50°C (held for 3 minutes) and then programmed to a final temperature of 325 °C (held for 20 minutes) with an increase of 6 °C minutes^{-1}. To quantify the sterols we used nonadecanol and DAGE-18 with a known amount (10 ng µL) as external standards, with precision of 5.6 % and 4.9 %, respectively. To identify the sterols the mass spectra of each sample were investigated using a Thermo Scientific Trace GC Ultra coupled to a Thermo Scientific DSQ II mass spectrometer (GC-MS). He (2 mL minute^{-1} flow rate) was used as carrier gas. The initial GC temperature was 50 °C (held for 3 minutes) and ramped with 6 °C minute^{-1} to 325 °C (held for 25 minutes). The mass spectra of the compounds were then compared with published mass spectral data.

For major four phytoplankton groups, brassicasterol, dinosterol, dinostanol and C_{37} alkenone were used. For zooplankton cholesterol, and its degradative product cholestanol (Wittenborn et al., 2020) was used.

2.2.4 Sea surface temperature (SST) from satellite imagery

The SST data was accessed from the climate reanalysis version 5 (ERA5) of the European Centre for Medium-Range Weather Forecasts (ECMWF) (C3S, 2017). ERA5 covers the time from 1979 to the present at a 0.25° × 0.25° grid. In this study, we used monthly mean of SST data covering a period from 2017–2020 (downloaded from: https://cds.climate.copernicus.eu/cdsapp#!/dataset/reanalysis-era5-single-levels?tab=form.

2.2.5 Statistical analysis

The Shapiro-Wilk normality test and F test were used to check the normality and variance of individual datasets, respectively. The statistical significance between differences for various parameters was obtained using Single-factor Analysis of Variance (ANOVA) in Microsoft Excel at a 95% confidence level (probability p<0.05). The relationships between biotic (biomarkers, frustules, radiolarian, diatom community) and environmental (SST, TOC, TN, TIC, TOC:TN) variables were conducted using the CANOCO version 4.5 software (Ter Braak and Šmilauer, 2002). For explaining the correlation between the biotic and environmental variables a linear multivariate model RDA (Redundancy Analysis) was used.

3. Results

The sedimentary characteristics (TIC, TOC, TN), diatom frustule abundance, and diversity including radiolarian abundance from the top 0–0.5 cm were already published earlier (Pandey et al., 2023). In this study, we have analyzed the samples from 0.5–1 cm sediment depth and collectively shown an average representing the top 1 cm of the surface sediment (Table 1). Results of lipid biomarkers (0–0.5 and 0.5–1 cm) such as various phytosterols and the summed $C_{37:2}$ and $C_{37:3}$ alkenones as well as $U^{k'}_{37}$-derived sea surface temperature (SST) proxy are shown in Table 1. For further discussion of our results, the study area has been defined in two areas as the northern part (north of mean position of Findlater Jet) includes the sites 21, 19 and 15º N, whereas the southern part includes the sites 11, and 13 ºN (Fig. 1a).

3.1 Bulk sedimentary analysis and SST reconstruction

To compare with $U^{k'}_{37}$ based-SST reconstruction, we also present ~~here~~ the SST values derived from the satellite (Fig. 1b) averaged for the ~~last three~~ years ~~(~~2017–2020~~). Assuming~~ that the surface sediment usually represents the signature of recent time SST. High spatial variability in SST was observed from the north (mean 27.2°C) to the south (28°C). TIC contents (Fig. 2a) were slightly higher in the south (7.06 ± 0.63 %) compared to the north (5.15 ± 1.57 %) and this difference was statistically significant at a 94.7 % confidence level (single factor ANOVA analysis, Table 2). TOC contents (Fig. 2b) were substantially higher (p <0.001) above 15° N

https://doi.org/10.5194/egusphere-2024-845
Preprint. Discussion started: 24 April 2024

(0.97 ± 0.06 %) reaching their highest value at 21° N and decreased southward (0.78 ± 0.005 %). TN values (Fig. 2c) revealed a similar trend as TOC and decreased from 21° N (0.11 ± 0.001 %) to 11° N (0.07 ± 0.009 %). The average TN value (0.06 ± 0.008 %) in the south was significantly lower (p <0.001) compared to the north (0.087 ± 0.018 %). The ratio of TOC and TN (Table 1) was the lowest (9.5 ± 0.18) in the north at 21° N and increased at the rest of the stations reaching >12. The $U_{37}^{k'}$ based SST (Fig. 2d) shows an average value of 27.8 ± 0.3 °C. The coolest reconstructed SSTs (27.6 ± 0.25 °C) were found in the north and were nearly 0.4 °C cooler compared to the south (p =0.043) (Table 2).

3.2 Lipid biomarkers

The lipid biomarkers brassicasterol (diatoms) (Fig. 2e), dinosterol (dinoflagellates) (Fig. 2f), dinostanol, the saturated, degradative product of dinosterol (Fig. 2g), and summed $C_{37:2 \text{ and } 37:3}$ alkenones (C_{37} alkenone) (coccolithophores) (Fig. 2h) were present from north to south. The average dinosterol contents (98 ± 64 ng g^{-1}) found in the surface sediment were the highest of the biomarkers followed by brassicasterol (64 ± 44 ng g^{-1}) and C_{37} alkenones (39.4 ± 12 ng g^{-1}) (Table 1). All studied lipid biomarkers showed significant linear positive correlations (R^2 =0.62–0.96, p< 0.05) with each other indicating their similar responses to environmental variables. Their concentrations were quite high at the northernmost station at 21° N (Fig. 2; Table 1) and decreased to their minimum values at 11° N. However, there were apparent trends of decrease from north to south of the sampling transect, but none of the biomarkers showed any statistically significant difference in their TOC normalized values between the stations. The sum of the major biomarkers grossly represents the major three phytoplankton groups, with the highest (33.9 ± 14.13 µg g^{-1} TOC) at 21° N compared to other stations (19.96 ± 9.5 µg g^{-1} TOC). The TOC normalized values of dinosterol (16.53 ± 8.3 µg g^{-1} TOC) and brassicasterol (12.37 ± 5.2 µg g^{-1} TOC) were the highest at the northernmost station and decreased southward. However, the average values of dinosterol (north: 12.81 ± 6.3 µg g^{-1} TOC; south 7.8 ± 4.47 µg g^{-1} TOC) and brassicasterol (north: 8.64 ± 4.75 µg g^{-1} TOC; south 5.81 ± 3.48 µg g^{-1} TOC) were not significantly different (p>0.05) (Table 2). The average ratios of dinosterol to brassicasterol and brassicasterol to alkenones were 1.5 and 1.6 (Table 1), respectively, without any significant north-south variability (Table 2).

3.3 Zooplankton proxies

We used two proxies representing zooplankton: 1) sterol biomarker (cholesterol (Fig. 2i), and its degradative product cholestanol (Fig. 2j)), although it may come from some other sources (Wittenborn et al., 2020) and 2) radiolarians. Cholesterol, mostly varied between 10 ± 2.5 µg g^{-1} TOC (north) and 14.3 ± 5.8 µg g^{-1} TOC (south) without any statistical significance. The TOC normalized values of cholestanol are lower in the northern (11.8 ± 6.3 µg g^{-1} TOC) than in the southern part (15.9 ± 11.4 µg g^{-1} TOC) and no significant correlation was noticed (Table 2).

Radiolarian abundance (Fig. 2k) in the central Arabian Sea varied between 1.07 and 2.13 × 10^4 individuals g^{-1} with the highest numbers at 13° N and the lowest at 21° N. Their occurrences were found to be higher at the southern stations (1.84 × 10^4 individuals g^{-1}) compared to northern stations (1.10 × 10^4 individuals g^{-1}) with statistical significance (p<0.014) (Table 2). The community was dominated by the genus *Tetrapyle* sp. and their abundance was higher in the south.

3.4 Diatom frustules: abundance and diversity

Diatoms frustules from the surface sediment showed high spatial variability in both abundance and diversity. The total frustule abundance in the central Arabian Sea (Supplementary Table 1;

https://doi.org/10.5194/egusphere-2024-845
Preprint. Discussion started: 24 April 2024

Fig. 2l) ranged between 2.78 and 6.36 × 10^4 valves g^{-1}. The highest frustule abundance was observed at 19–21° N and the least at 11° N. At station 19° N, the frustule abundance was the highest (6.36 ± 0.2 × 10^4 valves g^{-1}) among all stations (Table 1). The frustule numbers found in the north (5.46 ± 0.95 × 10^4 valves g^{-1}) were 1.67 times higher than in the south (p=0.009). Diatom frustule diversity was calculated to understand the north-south distribution pattern and the average Shannon–Wiener diversity index (H′) was 1.6 ± 0.1 with the highest diversity at 21° N (1.8) (Supplementary Fig. 1). Microscopic analysis revealed a total of 23 genera, with 9 centric and 14 pennate diatoms. More than five-fold higher abundance of centric diatoms was observed than pennate at all the locations ($p < 0.05$). The abundance of pennate diatoms was higher towards southern stations without any statistical significance.

The overall diatom community in the sediment samples from the central Arabian Sea (Supplementary Table 1; Fig. 3) was observed to be dominated by *Coscinodiscus* (40%), *Thalassiosira* (34%), *Pseudo-nitzschia* (6%), *Rhizosolenia* (4%), *Hemidiscus* (4%), *Thalassionema* (4%), and *Nitzschia* (3%). The northern stations were dominated by *Coscinodiscus* sp., whereas the two southernmost stations were dominated by *Thalassiosira* sp. In the north, the highest abundance (2.46 × 10^4 valves g^{-1}) of *Coscinodiscus* sp. was observed (p< 0.05) with the least abundance at 11° N (0.61 × 10^4 valves g^{-1}). In the south, *Thalassiosira* seemed to dominate (1.59 × 10^4 valves g^{-1}) without any statistical significance. The Bray-Curtis similarity index usually indicates the similarity in the distribution pattern of different diatom genera/species. The results revealed (Supplementary Fig. 2) that the two dominating diatom genera, i.e. *Coscinodiscus* sp. and *Thalassiosira* sp were grouped showing a similar distribution pattern. The commonly occurring pennate diatom *Pseudo-nitzschia* was present independently, whereas *Rhizosolenia* and *Thalassionema* were clubbed. The other two major contributing diatom genera, *Hemidiscus* and *Nitzschia* revealed a similar pattern.

3.5 Statistical Analysis

In the RDA biplot (Fig. 4), Axis 1 and 2 explained most of the variability (~97.2%). The biotic variables and abiotic variables show a distinct association. Interestingly, TOC, TN, the key phytoplankton biomarkers (dinosterol, brassicasterol, dinostanol, and alkenones), along with diatom frustules abundance, and the major genera were clubbed and were at the opposite axis where TIC, SST, cholesterol, and radiolarian were together. The association between the larger diatoms like *Coscinodiscus* and *Rhizosolenia* and organic matter including brassicasterol depicted that the organic matter flux was coupled with diatom fluxes. The positioning of *Thalassiosira* opposite these parameters also suggested that its abundance was higher in the south associated with warmer SSTs. TOC:TN ratio and TIC along with SST were together.

4. Discussion

4.1 Physical Forcing induced spatial variability in physicochemical properties

The alkenone-derived SST suggested a cooler northern part (19–21° N) compared to the south along the sampling transect (64° E, Fig. 2d). The annual average of satellite-derived SST also revealed a similar trend. Such variability in SST from north to south could be attributed to monsoon wind variability and related processes. During the summer monsoon, the physicochemical parameters (wind speed, SST, nutrients, mixed layer depths [MLDs]) along 64° E show distinct north-south demarcation due to the presence of the Findlater Jet (Findlater, 1971). In the northern flank of this jet axis, the maximum influence of upwelling is evidenced by the presence of cooler SSTs, high nutrient levels, and shallower MLDs (Silori et al., 2021; Chowdhury et al., 2021; Chowdhury et al., 2024). Along the axis (~15–18° N) of the Jet the highest wind speeds are recorded (Silori et al., 2021; Chowdhury et al., 2021; Chowdhury et

https://doi.org/10.5194/egusphere-2024-845
Preprint. Discussion started: 24 April 2024

al., 2024). The coolest SST value at 15° N is most likely due to the advection of cool nutrient-rich upwelled waters from the western coastal Arabian Sea (Bauer et al., 1991). Furthermore, such high wind speeds for a prolonged period may also lead to evaporative heat loss leading to a decrease in SST. Contrarily, in the south downwelling induced deeper MLDs (>100 m), nutrient-poor waters along with higher SSTs are observed (Latasa and Bidigare, 1998; Chowdhury et al., 2021; Silori et al., 2021). During the winter monsoon, surface circulation reverses in this region, and in the northern Arabian Sea cold dry wind leads to evaporative cooling and subsequent convection leading to cooler SSTs, and high nutrient levels. At the same time, southern regions remain oligotrophic and warm. During the intermonsoon and premonsoon, SST increases and nutrient level reduces substantially along the entire transect (Prasannakumar and Narvekar, 2005).

4.2 Spatial variability in particle flux, and phytoplankton dynamics

4.2.1 Organic matter

The northernmost stations were the hotspots for particulate organic matter (POM) flux and sink to the sediment floor (Fig. 2). The positioning of SST in the RDA plot (Fig. 4) opposite TOC, TN, diatom frustules, and phytoplankton biomarkers also supported this fact. The north-south variability in phytodetritus flux could be also influenced by dissolved oxygen levels within the mesopelagic (Fig. 5) as it directly controls microbial degradation and zooplankton activity (Moriceau et al., 2018; Iversen, 2023). In our sampling transect, the northern stations are under the influence of intense OMZ and the intensity as well as the thickness reduces while moving southward (Banse et al., 2014). In their synthesis, Banse et al. (2014) showed that the median DO values within 150–500 m depth in the northern stations within the core OMZ vary between 0.04 and 0.30 mL L^{-1}. Conversely, in the south, these values increased to 0.24–0.72 mL L^{-1}. Such spatial variability in OMZ distribution/intensity across the stations could substantially alter the rate of organic matter mineralization, zooplankton abundance (Cavan et al., 2017), and particle flux attenuation (François et al., 2002; Keil et al., 2016). Fast and efficient mineralization within the mesopelagic may allow less organic matter to be transported, whereas partial remineralization may lead to higher organic matter export flux (Ragueneau et al., 2006). Therefore, the northern station with an intense OMZ may have a higher preservation potential of organic matter compared to the south (Fig. 5) as mentioned by Schulte et al. (2000).

4.2.2 Phytoplankton biomarkers

TOC-normalized lipid biomarker contents collected from the surface sediment represent the relative contribution of individual phytoplankton groups to total organic matter transfer from the upper oceanic layers to the deep sea floor. In this study, total and TOC-normalized phytoplankton biomarkers revealed that dinoflagellates, diatoms, and coccolithophores were the dominant phytoplankton groups transferring carbon to the surface sediment (Fig. 2). All studies available from the Arabian Sea using biomarkers (Schubert et al., 1998; Schulte et al., 1999; 2000; Prahl et al., 2000) showed that dinosterol contents were higher than brassicasterol, both in sediment core and trap samples, suggesting greater contributions of dinoflagellates compared to diatoms. In this study, nearly 1.5 times higher dinosterol contents compared to brassicasterol all along the transect also confirmed this. Likewise, the dominance of dinosterol, C_{37}-alkenones, and some species-specific biomarkers for diatoms was found in sediment trap samples (2220 m depth) from the Central Arabian Sea (Prahl et al., 2000), in two sediment core samples from the northeastern and southern Arabian Sea (Schulte et al., 1999). Further, a long sediment core from the northern Arabian Sea close to our sampling locations (22° 29.31′ N,

https://doi.org/10.5194/egusphere-2024-845
Preprint. Discussion started: 24 April 2024

65° 38.9′ E) (Schubert et al., 1998) reported about the same dominating phytoplankton groups in the Arabian Sea over the past 0.2 million years.

Since diatoms predominate over dinoflagellates during phytoplankton blooms (Chowdhury et al., 2021; 2024) a higher contribution of brassicasterol over dinosterol can be expected, however, it was the opposite in our study. This reverse trend can be explained by the seasonal succession of phytoplankton communities in surface layers mostly driven by nutrient stoichiometry related to monsoon wind forcings and grazing (Prahl et al., 2000; Rixen et al., 2019a). It should be noted that organic matter on the surface sediment accumulates throughout the year with variable depositional rates. Monsoon reversal also leads to changes in the phytoplankton community (Sawant and Madhupratap, 1996; Latasa and Bidigare, 1998) that may also affect the transfer of phytodetritus to the sea floor. Consequently, diatom frustules largely represent the signature of the most productive periods. However, the nutrient-poor phases are usually dominated by dinoflagellates and other calcifying nanophytoplankton. Dinoflagellates grow slowly in nutrient-poor warm waters and can remain there for longer periods (k-strategists) (Smayda and Reynolds, 2001; Glibert et al., 2016). Likewise, this situation can be compared to the southern stations, where high SSTs and oligotrophic conditions were more favorable for the growth of dinoflagellates (Chowdhury et al., 2021; 2024). This is reflected south of the 15° N station by the occurrences of dinoflagellates like *Gymnodinium* sp. *Gyrodinium* sp, and *Katodinium* sp. with small cells (Garrison et al., 1998; Chowdhury et al., 2021).

Moreover, unlike diatoms, which are autotrophs, most dinoflagellates could be either heterotrophs or mixotrophs (Stoecker, 1999; Stoecker et al., 2017) which actively graze on smaller phytoplankton including diatoms and even could be detritivorous feeding on particles (García-Oliva et al., 2022). Mixotrophs could consume prey to meet their cellular nitrogen demand and can simultaneously perform photosynthesis to gain carbon (Stoecker et al., 2017). In the Arabian Sea dissolved inorganic nitrogen is the limiting nutrient and a significant part of the available nitrogen is lost due to strong denitrification within the OMZ (Ward et al., 2006). Therefore, particularly during the stratified oligotrophic phases like intermonsoon and premonsoon, when SST increases ~~follow~~ed ~~by~~ stratification, nanophytoplankton, and dinoflagellates dominate over diatoms. Hence, the overall contribution of dinoflagellates on an annual basis could exceed diatoms as dinoflagellates are constantly present during both high-nutrient regimes and low-nutrient stratified warm water periods.

Another possible factor for the observed variability in brassicasterol to dinosterol could be due to differences in their labile nature. It was claimed that diatom-rich organic matter could be of higher lability (François et al., 2002) and may possess low transfer potential to the sea floor (Alonso-González et al., 2010). Contrary to this, it was ~~also~~ observed that compared to other phytoplankton (Cabrera-Brufau et al., 2021) diatom-rich organic matter is more of a refractory nature against mesopelagic microbial degradation. Moreover, the phytodetritus of diatom origin could be preferably e[illegible] by the benthic communities than other phytoplankton groups (Nomaki et al., 2021) and co[illegible] be one of the reasons for lower brassicasterol over dinosterol in the surface sediment. This is indeed difficult to conclude as we do not have enough experimental evidence supporting/contradicting these hypotheses.

In the central Arabian Sea, coccolithophores constitute an important part of the nanophytoplankton community (Andruleit et al., 2004; Mergulhao et al., 2006). The relatively high occurrences of substantial amounts of C_{37}-alkenones all along the transect in our study indicate that coccolithophores may also contribute as a major part of sinking phytodetritus, with slightly higher values towards the north (Fig. 2h). Sediment trap studies from the south of

https://doi.org/10.5194/egusphere-2024-845
Preprint. Discussion started: 24 April 2024

the Findlater Jet (Mergulhao et al., 2006) reported the flux of coccolithophores throughout the year justifying our observations.

4.2.3 Diatom frustules

The highest abundance of diatom frustules coupled with TOC and TN contents were found in the northern stations (19-21° N), which most likely indicated higher organic matter transfer to the sediment compared to the southern stations. The RDA plot (Fig. 4) also revealed that the abundance of large centric diatoms like *Coscinodiscus, Rhizosolenia,* TOC, and TN contents as well as brassicasterol were grouped and correlated significantly. During both summer (Chowdhury et al., 2021) and winter monsoons (Sawant and Madhupratap, 1996) in the northern Arabian Sea, *Coscinodiscus* and *Rhizosolenia* are the major diatoms forming blooms and consequently, dominate the particle flux (opal/biogenic silica) (Rixen et al., 2019a). A higher abundance of large *Rhizosolenia* frustules was also seen in the sediment trap samples from the central Arabian Sea after the summer monsoon ~~bloom~~ (Rixen et al., 2019a). The contribution of heavily silicified diatom frustules may in addition provide ballasting effects (Smetacek, 1985; Tréguer et al., 2018) facilitating efficient organic matter export compared to other phytoplankton groups (Buesseler, 1998; Boyd and Newton, 1999; Zúñiga et al., 2021). Diatom bloom development in the Arabian Sea was found to be associated with dissolved silica (DSi) availability (Chowdhury et al., 2021) and the depth of the silicicline (Anju et al., 2020). The northern stations become DSi depleted (<2 µM) at the end of the bloom (Chowdhury et al., 2021) and may lead to a mass sinking of frustules (Smetacek, 1985; Krause et al., 2019) or they can be grazed and cell death may also occur due to viral attacks (Agusti and Duarte, 2000). On the other hand, the abundance of small chain-forming diatoms such as *Thalassiosira*, *Pseudo-nitzschia*, *Nitzschia,* and *Thalassionema*~~,~~ enhanced in the surface sediment in the southern stations (Fig. 3) low nutrient conditions prevail even during summer and winter monsoons. During the intermonsoon and premonsoon oligotrophy intensifies in these regions supporting the growth of smaller diatoms or non-diatoms (Garrison et al., 1998; Tarran et al., 1999; Chowdhury et al., 2021) that could sink slower compared to the larger cells in the north (Buesseler and Boyd, 2009).

Moreover, diatom frustules may dissolve while sinking and ~~usually the thickly~~ silicified frustules reach the abyssal plain and ~~can be well preserved~~. Nevertheless, the organic coating that protects siliceous frustules from dissolution (Lewin, 1961)~~,~~ can be degraded by heterotrophic bacterial activity (Bidle and Azam, 1999; Roubeix et al., 2008). The presence of OMZ in the northern stations (200–1200m) could therefore slow down such dissolution facilitating frustules to reach the sea floor. On the other hand, in the south, small and thinly silicified diatom frustules (mostly due to DSi limitation) may be more fragile as they travel through the well-oxygenated water column and higher heterotrophic activity may enhance the risk of ~~dissolution~~ leading to reduced frustules abundance on the seabed. In addition to this, the almost 700 m deeper water column in the south compared to the north could enhance the scope of degradation of sinking particles. This is consistent with our observation.

4.2.4 Zooplankton grazing

The highest concentration of TOC-normalized cholesterol was found in the south indicating more zooplankton activity. In the RDA biplot, SST was clubbed with cholestanol and was on the same side of cholesterol indicating higher zooplankton activity in the south. The association of TIC with cholesterol indicates that calcareous zooplankton could also be a source of cholesterol. Consequently, a higher fecal matter production could enhance particle flux compared to the north. Nonetheless, a major part of the fecal matter could also be degraded within the upper mesopelagic layer as reported by Iversen et al. (2017). The authors observed

https://doi.org/10.5194/egusphere-2024-845
Preprint. Discussion started: 24 April 2024

that more than 87% of fecal matter produced in the surface ocean can be lost via remineralization before reaching upper mesopelagic (300 m) in the Southern Ocean. Likewise, the warmer temperature in the mesopelagic of our study location could facilitate faster mineralization. Zooplankton grazing could largely alter the magnitude of carbon export flux (Moriceau et al., 2018). Thus, the low abundance of mesozooplankton within the OMZ may decrease defragmentation which in turn slows down the bacterial remineralization of phytodetritus allowing a higher amount of carbon to be exported to the abyssal plain (Cavan et al., 2017) (Fig. 5). Likewise, the lower zooplankton activity in the mesopelagic ~~within the~~ OMZ of the Arabian Sea (Wishner et al., 1998) may hinder particle fragmentation that usually accelerates degradation (Briggs et al., 2020). Likewise, at the northern stations, lower zooplankton abundance within the OMZ (Cavan et al., 2017) may restrict particle flux attenuation (Fig. 5).

In the western and central Arabian Sea, ~~nearly~~ 50–100% of the diatom population can be grazed by copepods (Landry et al., 1998; Smith et al., 1998; Gauns et al., 2005). Importantly, diatom cell size can be a crucial factor that determines their grazing rates. Copepods exhibit the highest grazing rate when the ratio between prey and predator body size remains 18:1 on average (Hansen et al., 1994). In the north and at the axis of the Findlater Jet, the higher availability of nutrients, particularly DSi could promote large and thickly silicified diatoms which are difficult to graze for copepods (Hansen et al., 1994; Ryderheim et al., 2022). Subsequently, large centric diatoms like *Coscinodiscus radiatus* and *Rhizosolenia* spp. could escape grazing by copepods (Jansen, 2008; Löder et al., 2011) and can sink to the sediment floor (Buesseler and Boyd, 2009; Kemp et al., 2006). On the contrary, the bloom-forming diatoms with thinly silicified frustules like *Chaetoceros* and *Leptocylindrus* (Sawant and Madhupratap, 1996; Chowdhury et al., 2021) can be grazed easily and are usually not found in the sediment. However, the organic signature can be reflected in sedimentary biomarkers like brassicasterol. In the case of southern stations, smaller diatoms or non-diatoms could be consumed by microzooplankton (Swanberg and Anderson, 1985). Corroborating with this fact, the significantly higher number of radiolarians (Fig. 2k) which mostly consume smaller phytoplankton, bacterioplankton, and copepods (Caron et al., 1995) were higher in the south. A high abundance of radiolarians dominated by *Tetrapyle sp.* that are found under high salinity was also reported by a previous study from the Arabian Sea (Gupta, 2003).

4.2.5 Influence of lateral advection

Since there is evidence of advected waters reaching from the western Arabian Sea to its central part, the chances of particle transport also need to be considered. Nitrogen-stable isotopic values of particulate organic matter ($\delta^{15}N_{POM,}$ Silori et al. 2021) revealed that nutrient enrichment mostly takes place via advection from the upwelling system as well as entrainment close to the axis (16-18° N). Earlier studies also noticed the presence of slightly low saline waters in this region probably due to advection from the western Arabian Sea (Prasanna Kumar et al., 2000). Additionally, Silori et al. (2021) reported lower $\delta^{15}N$ values of particulate nitrogen during summer monsoon at the stations influenced by the axis suggesting laterally advected dissolved inorganic nitrogen from the Somali upwelling region. However, so far there is no report claiming that particulate organic matter can be advected such a long distance (~600 km) without being grazed/remineralized/sinking. Contrarily, there is plenty of evidence showing a direct relation between phytoplankton bloom and particle flux in these regions (Haake et al., 1993; Rixen et al., 2019a). Thus, the possibility of lateral transport of phytoplankton or detritus from the western Arabian Sea to the seabed of the central Arabian Sea may be partly overruled.

https://doi.org/10.5194/egusphere-2024-845
Preprint. Discussion started: 24 April 2024

Conclusions

This study aims for the first time to elucidate phytoplankton-driven particle flux to the sea floor using sedimentary organic biomarkers from the central Arabian Sea. Such studies linking sedimentary organic matter to physical forcings and phytoplankton community have rarely been studied in the central Arabian Sea. Importantly, most of the studies using sediment traps focused on diatoms and coccolithophores, but neglected dinoflagellates (Nair et al., 1989). A few studies proposed that the diatom blooms could be replaced by dinoflagellates. On the other hand, another study (Schubert et al. 1998), revealed that the relative contribution of dinosterol was higher than brassicasterol over the last 0.2 million years in this basin. Following this concept, we crosschecked the organic matter from the top 1 cm of surface sediments from more locations across a spatially variable transect (from high to low productive). Our results also indicated that dinoflagellates have contributed more to the sedimentary phytodetritus compared to diatoms even in the recent past. We propose that diatoms and coccolithophores do contribute to sedimentary particle flux. However, the dinoflagellates dominate due to their smart survival strategies during poor nutrient supply. We show that the distinct spatial variability in physical forcing drives the phytoplankton bloom and the particle flux is also closely coupled with this fact. The northernmost station in the central Arabian Sea was found to be a hotspot for sinking particles followed by subsequent preservation mostly due to the prevailing OMZ (Fig. 5). Both summer and winter monsoon-induced phytoplankton bloom dominated by diatoms led to the sinking of large thickly silicifed frustule on the sediment floor. We hypothesized that the low oxygen within the thick OMZ could slow down the dissolution of frustules as well as heterotrophic degradation and fragmentation by zooplankton leading to low flux attenuation. Contrarily, in the south, higher dissolved oxygen levels could facilitate faster remineralization and higher zooplankton activity resulting in more flux attenuation and reduced particle transport to the sea floor. Contrary to the global scenario of expanding OMZ, a recent modeling study (Vallivattathillam et al., 2023) showed that the southern part of the OMZ can get thinner in the future due to the higher supply of oxygen. Such changes could facilitate higher heterotrophic activities within the mesopelagic and thus could impact particle flux attenuation in this region and need to be investigated.

Acknowledgments

MP was supported by the Department of Science and Technology (DST) - Inspire Fellowship. This study is an outcome of CSIR-NIO in-house program “Impact of Climate Change on the Physics, Biogeochemistry, and the Ecology of the North Indian Ocean (CliCNIO)” (MLP 1802) funded by the Council of Scientific and Industrial Research (CSIR). We express out gratitude to the captain, scientists, technical staff, ship cell staff, deckhands, and the students onboard RV Sindhu Sadhana (SSD 068) for their constant help and support during the cruise. We are thankful to the Director, CSIR NIO for his kind support. Ms. Teja Naik is acknowledged for ~~th~~ technical help in using the Coulometer under the central analytical facility in CSIR, NIO, ~~G~~a. The contribution number is XXXX. NB was funded by the Deutsche Forschungsgemeinschaft (DFG, German Research Foundation) under Germany‘s Excellence Strategy – EXC 2037 'CLICCS - Climate, Climatic Change, and Society' – Project Number: 390683824, contribution to the Center for Earth System Research and Sustainability (CEN) of Universität Hamburg. The ~~aut~~ ~~s~~) wish to acknowledge use of the Ferret program for analysis and graphics in this paper. Ferret is a product of NOAA's Pacific Marine Environmental Laboratory. (Information is available at http://ferret.pmel.noaa.gov/Ferret/).

Availability of data and materials: Data will be available on request

https://doi.org/10.5194/egusphere-2024-845
Preprint. Discussion started: 24 April 2024

Statements and Declarations

Competing Interests: *The authors have no relevant financial or non-financial interests to disclose.*

Ethical Approval: Not applicable

Consent to Participate: Not applicable

Consent to Publish: Not applicable

Authors' Contributions: *MP: Conceptualization, sampling, sample analysis; formal analysis, data curation, writing original manuscript and editing; HB: Conceptualization; Fund acquisition; sampling; manuscript reviewing and editing; DB: sampling; manuscript reviewing and editing NB: Sample analysis, Conceptualization; manuscript reviewing and editing BG: Conceptualization; reviewing and editing*

References

1. Abrantes, F.F.G. and Sancetta, C.: Diatom assemblages in surface sediments reflect coastal upwelling off southern Portugal, Oceanologica acta, 8,7–12, 1985.
2. Agustí, S. and Duarte, C.M.: Strong seasonality in phytoplankton cell lysis in the NW Mediterranean littoral, Limnology and Oceanography, 45, 940–947, https://doi.org/10.4319/lo.2000.45.4.0940, 2000.
3. Alonso-González, I.J., Arístegui, J., Lee, C., Sanchez-Vidal, A., Calafat, A., Fabrés, J., Sangrá, P., Masqué, P., Hernández-Guerra, A. and Benítez-Barrios, V.: Role of slowly settling particles in the ocean carbon cycle, Geophysical research letters, 37, https://doi.org/10.1029/2010GL043827, 2010.
4. Andruleit, H., Rogalla, U. and Stäger, S.: From living communities to fossil assemblages: origin and fate of coccolithophores in the northern Arabian Sea, Micropaleontology, 50, 5-21, https://doi.org/10.2113/50.Suppl_1.5, 2004.
5. Anju, M., Sreeush, M.G., Valsala, V., Smitha, B.R., Hamza, F., Bharathi, G. and Naidu, C.V.: Understanding the role of nutrient limitation on plankton biomass over Arabian Sea via 1-D coupled biogeochemical model and bio-Argo observations, Journal of Geophysical Research: Oceans, 125, e2019JC015502, https://doi.org/10.1029/2019JC015502, 2020.
6. Armbrecht, L.H., Lowe, V., Escutia, C., Iwai, M., McKay, R. and Armand, L.K.: Variability in diatom and silicoflagellate assemblages during mid-Pliocene glacial-interglacial cycles determined in Hole U1361A of IODP Expedition 318, Antarctic Wilkes Land Margin, Marine Micropaleontology, 139, 28–41, https://doi.org/10.1016/j.marmicro.2017.10.008, 2018.
7. Banse, K.: Seasonality of phytoplankton chlorophyll in the central and northern Arabian Sea, Deep Sea Research Part A, Oceanographic Research Papers, 34, 713–723, https://doi.org/10.1016/0198-0149(87)90032-X, 1987.
8. Banse, K., Naqvi, S.W.A., Narvekar, P.V., Postel, J.R. and Jayakumar, D.A.: Oxygen minimum zone of the open Arabian Sea: variability of oxygen and nitrite from daily to decadal timescales, Biogeosciences, 11, 2237–2261, https://doi.org/10.5194/bg-11-2237-2014, 2014.
9. Barnett, P.R.O., Watson, J. and Connelly, D.: A multiple corer for taking virtually undisturbed samples from shelf, bathyal and abyssal sediments, Oceanologica acta, 7, 399–408, 1984.
10. Bauer, S., Hitchcock, G.L., Olson, D.B.: Influence of monsoonally-forced Ekman dynamics upon surface layer depth and plankton biomass distribution in the Arabian

https://doi.org/10.5194/egusphere-2024-845
Preprint. Discussion started: 24 April 2024

Sea, Deep Sea Research, Part A Oceanographic Research Papers 38, 531–553, https://doi.org/10.1016/0198-0149(91)90062-K, 1991.

11. Behrenfeld, M.J., O'Malley, R.T., Siegel, D.A., McClain, C.R., Sarmiento, J.L., Feldman, G.C., Milligan, A.J., Falkowski, P.G., Letelier, R.M. and Boss, E.S.: Climate-driven trends in contemporary ocean productivity, Nature, 444,752–755, https://doi.org/10.1038/nature05317, 2006.
12. Bhattathiri, P.M.A., Pant, A., Sawant, S., Gauns, M., Matondkar, S.G.P. and Mohanraju, R.: Phytoplankton production and chlorophyll, Current Science, 71, 1996.
13. Bidle, K.D. and Azam, F.: Accelerated dissolution of diatom silica by marine bacterial assemblages, Nature, 397, 508–512, https://doi.org/10.1038/17351, 1999.
14. Boyd, P.W. and Newton, P.P.: Does planktonic community structure determine downward particulate organic carbon flux in different oceanic provinces?, Deep Sea Research Part I: Oceanographic Research Papers, 46, 63–91, https://doi.org/10.1016/S09670637(98)00066-1, 1999.
15. Briggs, N., Dall'Olmo, G. and Claustre, H.: Major role of particle fragmentation in regulating biological sequestration of CO_2 by the oceans, Science, 367, 791–793, https://doi.org/10.1126/science.aay1790, 2020.
16. Buesseler, K.O. and Boyd, P.W.: Shedding light on processes that control particle export and flux attenuation in the twilight zone of the open ocean, Limnology and Oceanography, 54, 1210–1232, https://doi.org/10.4319/lo.2009.54.4.1210, 2009.
17. Buesseler, K.O.: The decoupling of production and particulate export in the surface ocean, Global Biogeochemical Cycles, 12, 297–310, https://doi.org/10.1029/97GB03366, 1998.
18. Cabrera-Brufau, M., Arin, L., Sala, M.M., Cermeño, P. and Marrasé, C.: Diatom dominance enhances resistance of phytoplanktonic POM to mesopelagic microbial decomposition, Frontiers in Marine Science, 8, p.683354, https://doi.org/10.3389/fmars.2021.683354, 2021.
19. Caron, D.A., Michaels, A.F., Swanberg, N.R. and Howse, F.A.: Primary productivity by symbiont-bearing planktonic sarcodines (Acantharia, Radiolaria, Foraminifera) in surface waters near Bermuda, Journal of Plankton Research, 17, 103–129. https://doi.org/10.1093/plankt/17.1.103, 1995.
20. Cavan, E.L., Trimmer, M., Shelley, F. and Sanders, R.: Remineralization of particulate organic carbon in an ocean oxygen minimum zone. Nature Communications, 8(1), p.14847, https://doi.org/10.1038/ncomms14847, 2017.
21. Chowdhury, M., Biswas, H., Mitra, A., Silori, S., Sharma, D., Bandyopadhyay, D., Shaik, A.U.R., Fernandes, V. and Narvekar, J.: Southwest monsoon-driven changes in the phytoplankton community structure in the central Arabian Sea (2017–2018): After two decades of JGOFS, Progress in Oceanography, 197, p.102654, https://doi.org/10.1016/j.pocean.2021.102654, 2021.
22. Chowdhury, M., Biswas, H., Silori, S. and Sharma, D.: Spatiotemporal variability in phytoplankton size class modulated by summer monsoon wind forcing in the central Arabian Sea, Journal of Geophysical Research: Oceans, 129, e2023JC019880, https://doi.org/10.1029/2023JC019880, 2024.
23. Copernicus Climate Change Service (C3S), ERA5: Fifth generation of ECMWF atmospheric reanalyses of the global climate, Copernicus Climate Change Service Climate Data Store (CDS), 2017.
24. Desikachary, T.V.: Atlas of Diatoms (Marine Diatoms of the Indian Ocean Region), 6, Madras Science Foundation, Madras Fasc, 1–13, 1989.

https://doi.org/10.5194/egusphere-2024-845
Preprint. Discussion started: 24 April 2024

25. Engel, A., Wagner, H., Le Moigne, F.A. and Wilson, S.T.: Particle export fluxes to the oxygen minimum zone of the eastern tropical North Atlantic, Biogeosciences, 14,1825-1838, https://doi.org/10.5194/bg-14-1825-2017, 2017.
26. Field, C.B., Behrenfeld, M.J., Randerson, J.T. and Falkowski, P.: Primary production of the biosphere: integrating terrestrial and oceanic components, Science, 281, 237–240, https://doi.org/10.1126/science.281.5374.237, 1998.
27. Findlater, J.: Mean monthly airflow at low levels over the western Indian Ocean (No. 116). HM Stationery Office, Pure Appl. Geophys. PAGEOPH 115, 1251–1262, https://doi.org/10.1007/BF00874408, 1971.
28. Francois, R., Honjo, S., Krishfield, R. and Manganini, S.: Factors controlling the flux of organic carbon to the bathypelagic zone of the ocean, Global Biogeochemical Cycles, 16, 34–1, https://doi.org/10.1029/2001GB001722, 2002.
29. García-Oliva, O., Hantzsche, F.M., Boersma, M. and Wirtz, K.W.: Phytoplankton and particle size spectra indicate intense mixotrophic dinoflagellates grazing from summer to winter. Journal of Plankton Research, 44, 224–240, https://doi.org/10.1093/plankt/fbac013, 2022.
30. Garrison, D.L., Gowing, M.M. and Hughes, M.P.: Nano-and microplankton in the northern Arabian Sea during the Southwest Monsoon, August–September 1995 A US–JGOFS study, Deep Sea Research Part II: Topical Studies in Oceanography, 45, 2269–2299, https://doi.org/10.1016/S0967-0645(98)00071-X, 1998.
31. Gauns, M., Madhupratap, M., Ramaiah, N., Jyothibabu, R., Fernandes, V., Paul, J.T. and Kumar, S.P.: Comparative accounts of biological productivity characteristics and estimates of carbon fluxes in the Arabian Sea and the Bay of Bengal. Deep Sea Research Part II: Topical Studies in Oceanography, 52, 2003–2017, https://doi.org/10.1016/j.dsr2.2005.05.009, 2005.
32. Glibert, P.M., Wilkerson, F.P., Dugdale, R.C., Raven, J.A., Dupont, C.L., Leavitt, P.R., Parker, A.E., Burkholder, J.M. and Kana, T.M.: Pluses and minuses of ammonium and nitrate uptake and assimilation by phytoplankton and implications for productivity and community composition, with emphasis on nitrogen-enriched conditions, Limnology and Oceanography, 61, 165–197, https://doi.org/10.1002/lno.10203, 2016.
33. Gupta, S.M.: Orbital frequencies in radiolarian assemblages of the central Indian Ocean: implications on the Indian summer monsoon, Palaeogeography, Palaeoclimatology, Palaeoecology, 197(1-2), 97–112, https://doi.org/10.1016/S0031-0182(03)00388-2, 2003.
34. Haake, B., Ittekkot, V., Rixen, T., Ramaswamy, V., Nair, R.R. and Curry, W.B.: Seasonality and interannual variability of particle fluxes to the deep Arabian Sea, Deep Sea Research Part I: Oceanographic Research Papers, 40(7), 1323–1344, https://doi.org/10.1016/0967-0637(93)90114-I, 1993.
35. Hansen, B., Bjornsen, P.K. and Hansen, P.J.: The size ratio between planktonic predators and their prey, Limnology and oceanography, 39(2), 395–403, https://doi.org/10.4319/lo.1994.39.2.0395, 1994.
36. Hu, L., Liu, Y., Xiao, X., Gong, X., Zou, J., Bai, Y., Gorbarenko, S., Fahl, K., Stein, R. and Shi, X.: Sedimentary records of bulk organic matter and lipid biomarkers in the Bering Sea: A centennial perspective of sea-ice variability and phytoplankton community, Marine Geology, 429, 106308, https://doi.org/10.1016/j.margeo.2020.106308 , 2020.
37. Iversen, M.H., Pakhomov, E.A., Hunt, B.P., Van der Jagt, H., Wolf-Gladrow, D. and Klaas, C.: Sinkers or floaters? Contribution from salp pellets to the export flux during a large bloom event in the Southern Ocean, Deep Sea Research Part II: Topical Studies in Oceanography, 138, 116–125, https://doi.org/10.1016/j.dsr2.2016.12.004, 2017.

https://doi.org/10.5194/egusphere-2024-845
Preprint. Discussion started: 24 April 2024

38. Iversen, M.H.: Carbon Export in the Ocean: A Biologist's Perspective, Annual Review of Marine Science, 15, 357–381, 10.1146/annurev-marine-032122-035153, 2023.
39. Jansen, S.: Copepods grazing on Coscinodiscus wailesii: a question of size?, Helgoland Marine Research, 62(3), 251–255, https://doi.org/10.1007/s10152-008-0113-z, 2008.
40. Keil, R.G., Neibauer, J.A., Biladeau, C., van der Elst, K. and Devol, A.H.: A multiproxy approach to understanding the" enhanced" flux of organic matter through the oxygen-deficient waters of the Arabian Sea, Biogeosciences, 13(7), 2077–2092, https://doi.org/10.5194/bg-13-2077-2016, 2016.
41. Kemp, A.E., Pearce, R.B., Grigorov, I., Rance, J., Lange, C.B., Quilty, P. and Salter, I., Production of giant marine diatoms and their export at oceanic frontal zones: Implications for Si and C flux from stratified oceans, Global Biogeochemical Cycles, 20(4), https://doi.org/10.1029/2006GB002698, 2006.
42. Krause, J.W., Schulz, I.K., Rowe, K.A., Dobbins, W., Winding, M.H., Sejr, M.K., Duarte, C.M. and Agustí, S.: Silicic acid limitation drives bloom termination and potential carbon sequestration in an Arctic bloom, Scientific Reports, 9(1), 8149, https://doi.org/10.1038/s41598-019-44587-4, 2019.
43. Landry, M.R., Brown, S.L., Campbell, L., Constantinou, J. and Liu, H.: Spatial patterns in phytoplankton growth and microzooplankton grazing in the Arabian Sea during monsoon forcing, Deep Sea Research Part II: Topical Studies in Oceanography, 45(10–11), 2353–2368, https://doi.org/10.1016/S0967-0645(98)00074-5, 1998.
44. Latasa, M. and Bidigare, R.R.: A comparison of phytoplankton populations of the Arabian Sea during the Spring Intermonsoon and Southwest Monsoon of 1995 as described by HPLC-analyzed pigments, Deep Sea Research Part II: Topical Studies in Oceanography, 45(10-11), 2133–2170, https://doi.org/10.1016/S0967-0645(98)00066-6, 1998.
45. Le Moigne, F.A.: Pathways of organic carbon downward transport by the oceanic biological carbon pump, Frontiers in Marine Science, 6, 634, https://doi.org/10.3389/fmars.2019.00634, 2019.
46. Lewin, J.C.: The dissolution of silica from diatom walls, Geochimica et Cosmochimica Acta, 21(3-4), 182–198, https://doi.org/10.1016/S0016-7037(61)80054-9, 1961.
47. Liu, D., Shen, X., Di, B., Shi, Y., Keesing, J.K., Wang, Y. and Wang, Y.: Palaeoecological analysis of phytoplankton regime shifts in response to coastal eutrophication, Marine Ecology Progress Series, 475, 1–14, https://doi.org/10.3354/meps10234, 2013.
48. Löder, M.G., Meunier, C., Wiltshire, K.H., Boersma, M. and Aberle, N.: The role of ciliates, heterotrophic dinoflagellates and copepods in structuring spring plankton communities at Helgoland Roads, North Sea, Marine biology, 158, 1551–1580, https://doi.org/10.1007/s00227-011-1670-2, 2011.
49. Madhupratap, M., Kumar, S.P., Bhattathiri, P.M.A., Kumar, M.D., Raghukumar, S., Nair, K.K.C. and Ramaiah, N.: Mechanism of the biological response to winter cooling in the northeastern Arabian Sea, Nature, 384(6609), 549–552, https://doi.org/10.1038/384549a0, 1996.
50. Marsay, C.M., Sanders, R.J., Henson, S.A., Pabortsava, K., Achterberg, E.P. and Lampitt, R.S.: Attenuation of sinking particulate organic carbon flux through the mesopelagic ocean, Proceedings of the National Academy of Sciences, 112(4), 1089–1094, https://doi.org/10.1073/pnas.14153111, 2015.
51. McCreary, J.P., Murtugudde, R., Vialard, J., Vinayachandran, P.N., Wiggert, J.D., Hood, R.R., Shankar, D. and Shetye, S.: Biophysical processes in the Indian Ocean, Indian Ocean biogeochemical processes and ecological variability, 185, 9–32, https://doi.org/10.1029/2008GM000768, 2009.

https://doi.org/10.5194/egusphere-2024-845
Preprint. Discussion started: 24 April 2024

52. Mergulhao, L.P., Mohan, R., Murty, V.S.N., Guptha, M.V.S. and Sinha, D.K.: Coccolithophores from the central Arabian Sea: Sediment trap results, Journal of earth system science, 115, 415–428, https://doi.org/10.1007/BF02702870, 2006.
53. Moriceau, B., Iversen, M.H., Gallinari, M., Evertsen, A.J.O., Le Goff, M., Beker, B., Boutorh, J., Corvaisier, R., Coffineau, N., Donval, A. and Giering, S.L., Copepods boost the production but reduce the carbon export efficiency by diatoms, Frontiers in Marine Science, 5, 82, https://doi.org/10.3389/fmars.2018.00082, 2018.
54. Müller, J., Wagner, A., Fahl, K., Stein, R., Prange, M. and Lohmann, G.: Towards quantitative sea ice reconstructions in the northern North Atlantic: A combined biomarker and numerical modelling approach, Earth and Planetary Science Letters, 306(3-4), 137–148, https://doi.org/10.1016/j.epsl.2011.04.011, 2011.
55. Nair, R.R., Ittekkot, V., Manganini, S.J., Ramaswamy, V., Haake, B., Degens, E.T., Desai, B.T. and Honjo, S.: Increased particle flux to the deep ocean related to monsoons, Nature, 338(6218), 749–751, https://doi.org/10.1038/338749a0, 1989.
56. Nomaki, H., Rastelli, E., Ogawa, N.O., Matsui, Y., Tsuchiya, M., Manea, E., Corinaldesi, C., Hirai, M., Ohkouchi, N., Danovaro, R. and Nunoura, T.: In situ experimental evidences for responses of abyssal benthic biota to shifts in phytodetritus compositions linked to global climate change, Global Change Biology, 27(23), 6139–6155, https://doi.org/10.1111/gcb.15882, 2021.
57. Pandey, M., Biswas, H. and Chowdhury, M.: Interlinking diatom frustule diversity from the abyss of the central Arabian Sea to surface processes: physical forcing and oxygen minimum zone, Environmental Monitoring and Assessment, 195(1), 161, https://doi.org/10.1007/s10661-022-10749-7, 2023.
58. Pandey, M. and Biswas, H.: May. An account of the key diatom frustules from the surface sediments of the Central and Eastern Arabian Sea and their biogeochemical significance, In EGU General Assembly Conference Abstracts (EGU-131), https://doi.org/10.5194/egusphere-egu23-131, 2023.
59. Peng, P., Bi, R., Sachs, J.P., Shi, J., Luo, Y., Chen, W., Huh, C.A., Yu, M., Cao, Y., Wang, Y. and Cao, Z.: Phytoplankton community changes in a coastal upwelling system during the last century, Global and Planetary Change, 224, 104101, https://doi.org/10.1016/j.gloplacha.2023.104101, 2023.
60. Prahl, F. G., Muehlhausen, L. A. and Zahnle, D. L.: Further evaluation of long-chain alkenones as indicators of paleoceanographic conditions, Geochim. Cosmochim. Acta, 52(9), 2303–2310, doi:10.1016/0016-7037(88)90132-9, 1988.
61. Prahl, F.G., Dymond, J. and Sparrow, M.A.: Annual biomarker record for export production in the central Arabian Sea, Deep Sea Research Part II: Topical Studies in Oceanography, 47(7-8), 1581–1604, https://doi.org/10.1016/S0967-0645(99)00155-1, 2000.
62. Prasanna Kumar S., Madhupratap, M., Kumar, M.D., Gauns, M., Muraleedharan, P.M., Sarma, V.V.S.S. and De Souza, S.N.: Physical control of primary productivity on a seasonal scale in central and eastern Arabian Sea, Journal of Earth System Science, 109, 433–441, https://doi.org/10.1007/BF02708331, 2000.
63. Prasanna Kumar. S., and Narvekar, J.: Seasonal variability of the mixed layer in the central Arabian Sea and its implication on nutrients and primary productivity, Deep Sea Research Part II: Topical Studies in Oceanography, 52(14-15), 1848–1861, https://doi.org/10.1016/j.dsr2.2005.06.002, 2005.
64. Prasanna Kumar. S., Ramaiah, N., Gauns, M., Sarma, V.V.S.S., Muraleedharan, P.M., Raghukumar, S., Kumar, M.D. and Madhupratap, M.: Physical forcing of biological productivity in the Northern Arabian Sea during the Northeast Monsoon, Deep Sea

https://doi.org/10.5194/egusphere-2024-845
Preprint. Discussion started: 24 April 2024

Research Part II: Topical Studies in Oceanography, 48(6-7), 1115–1126, https://doi.org/10.1016/S0967-0645(00)00133-8, 2001.

65. Ragueneau, O., Schultes, S., Bidle, K., Claquin, P. and Moriceau, B.: Si and C interactions in the world ocean: Importance of ecological processes and implications for the role of diatoms in the biological pump, Global Biogeochemical Cycles, 20(4), https://doi.org/10.1029/2006GB002688, 2006.
66. Rixen, T., Gaye, B. and Emeis, K.C.: The monsoon, carbon fluxes, and the organic carbon pump in the northern Indian Ocean, Progress in oceanography, 175, 24–39, https://doi.org/10.1016/j.pocean.2019.03.001, 2019a.
67. Rixen, T., Gaye, B., Emeis, K.C. and Ramaswamy, V.: The ballast effect of lithogenic matter and its influences on the carbon fluxes in the Indian Ocean, Biogeosciences, 16(2), 485–503, https://doi.org/10.5194/bg-16-485-2019, 2019b.
68. Rodríguez-Miret, X., del Carmen Trapote, M., Sigró, J. and Vegas-Vilarrúbia, T.: Diatom responses to warming, heavy rains and human impact in a Mediterranean lake since the preindustrial period, Science of The Total Environment, 884, 163685, https://doi.org/10.1016/j.scitotenv.2023.163685, 2023.
69. Roubeix, V., Becquevort, S. and Lancelot, C.: Influence of bacteria and salinity on diatom biogenic silica dissolution in estuarine systems, Biogeochemistry, 88, 47–62, https://doi.org/10.1007/s10533-008-9193-8, 2008.
70. Roxy, M. K., Modi, A., Murtugudde, R., Valsala, V., Panickal, S., Kumar, S. P., Ravichandran, M., Vichi, M., and Levy, M.: A reduction in marine primary productivity driven by rapid warming over the tropical Indian Ocean, Geophysical Research Letters, 43, 826–833, https://doi.org/10.1002/2015GL066979, 2016.
71. Ryderheim, F., Grønning, J. and Kiørboe, T.: Thicker shells reduce copepod grazing on diatoms, Limnology and Oceanography Letters, 7(5), 435–442, https://doi.org/10.1002/lol2.10243, 2022.
72. Sawant, S. and Madhupratap, M.: Seasonality and composition of phytoplankton. Current Science, 71(11), 1996.
73. Schubert, C.J., Villanueva, J., Calvert, S.E., Cowie, G.L., Von Rad, U., Schulz, H., Berner, U. and Erlenkeuser, H.: Stable phytoplankton community structure in the Arabian Sea over the past 200,000 years, Nature, 394(6693), 563–566, https://doi.org/10.1038/29047, 1998.
74. Schulte, S., Mangelsdorf, K. and Rullkötter, J.: Organic matter preservation on the Pakistan continental margin as revealed by biomarker geochemistry, Organic Geochemistry, 31(10), 1005–1022, https://doi.org/10.1016/S0146-6380(00)00108-X, 2000.
75. Schulte, S., Rostek, F., Bard, E., Rullkötter, J. and Marchal, O.: Variations of oxygen-minimum and primary productivity recorded in sediments of the Arabian Sea, Earth and Planetary Science Letters, 173(3), 205–221, https://doi.org/10.1016/S0012-821X(99)00232-0, 1999.
76. Sharma, S., Ha, K.-J., Yamaguchi, R., Rodgers, K. B., Timmermann, A., and Chung, E.: Future Indian Ocean warming patterns, Nature Communications, 14, 1789, https://doi.org/10.1038/s41467-023-37435-7, 2023
77. Silori, S., Sharma, D., Chowdhury, M., Biswas, H., Cardinal, D. and Mandeng-Yogo, M.: Particulate organic matter dynamics and its isotopic signatures (δ13CPOC and δ15NPN) in relation to physical forcing in the central Arabian Sea during SW monsoon (2017–2018), Science of the Total Environment, 785, 147326, https://doi.org/10.1016/j.scitotenv.2021.147326, 2021.

https://doi.org/10.5194/egusphere-2024-845
Preprint. Discussion started: 24 April 2024

78. Singh, U.B. and Ahluwalia, A.S.: Microalgae: a promising tool for carbon sequestration, Mitigation and Adaptation Strategies for Global Change, 18(1), 73–95, https://doi.org/10.1007/s11027-012-9393-3, 2013.
79. Smayda, T.J. and Reynolds, C.S.: Community assembly in marine phytoplankton: application of recent models to harmful dinoflagellate blooms, Journal of plankton research, 23(5), 447–461, https://doi.org/10.1093/plankt/23.5.447, 2001.
80. Smetacek, V.S.: Role of sinking in diatom life-history cycles: ecological, evolutionary and geological significance, Marine biology, 84, 239–251, https://doi.org/10.1007/BF00392493, 1985.
81. Smith, S., Roman, M., Prusova, I., Wishner, K., Gowing, M., Codispoti, L.A., Barber, R., Marra, J. and Flagg, C.: Seasonal response of zooplankton to monsoonal reversals in the Arabian Sea, Deep Sea Research Part II: Topical Studies in Oceanography, 45(10-11), 2369–2403, https://doi.org/10.1016/S0967-0645(98)00075-7, 1998.
82. Sonzogni, C., Bard, E., Rostek, F., Lafont, R., Rosell-Mele, A. and Eglinton, G.: Core-top calibration of the alkenone index vs sea surface temperature in the Indian Ocean, Deep Sea Res. Part II Top. Stud. Oceanogr., 44(6), 1445–1460, doi:10.1016/S0967-0645(97)00010-6, 1997.
83. Stoecker, D.K.: Mixotrophy among Dinoflagellates 1. Journal of eukaryotic microbiology, 46, 397-401, https://doi.org/10.1111/j.1550-7408.1999.tb04619.x, 1999.
84. Stoecker, D.K., Hansen, P.J., Caron, D.A. and Mitra, A.: Mixotrophy in the marine plankton, Annual Review of Marine Science, 9, 311–335, https://doi.org/10.1146/annurev-marine-010816-060617, 2017.
85. Swanberg, N.R. and Anderson, O.R.: The nutrition of radiolarians: Trophic activity of some solitary Spumellaria 1, Limnology and Oceanography, 30, 646–652, https://doi.org/10.4319/lo.1985.30.3.0646, 1985.
86. Tarran, G.A., Burkill, P.H., Edwards, E.S. and Woodward, E.M.S.: Phytoplankton community structure in the Arabian Sea during and after the SW monsoon, 1994, Deep Sea Research Part II: Topical Studies in Oceanography, 46, 655–676, https://doi.org/10.1016/S0967-0645(98)00122-2, 1999.
87. Ter Braak, C.J. and Smilauer, P.: CANOCO reference manual and CanoDraw for Windows user's guide: software for canonical community ordination (version 4.5), www. canoco. com, 2002.
88. Tomas, C. R., (Ed.), Identifying marine phytoplankton. Elsevier, 1997.
89. Tréguer, P., Bowler, C., Moriceau, B., Dutkiewicz, S., Gehlen, M., Aumont, O., Bittner, L., Dugdale, R., Finkel, Z., Iudicone, D. and Jahn, O.: Influence of diatom diversity on the ocean biological carbon pump, Nature Geoscience, 11, 27–37, https://doi.org/10.1038/s41561-017-0028-x, 2018.
90. Vallivattathillam, P., Lachkar, Z. and Lévy, M.: Shrinking of the Arabian Sea oxygen minimum zone with climate change projected with a downscaled model, Frontiers in Marine Science, 10, 1123739, https://doi.org/10.3389/fmars.2023.1123739, 2023.
91. Volk, T. and Hoffert, M.I.: Ocean carbon pumps: Analysis of relative strengths and efficiencies in ocean-driven atmospheric CO_2 changes, The carbon cycle and atmospheric CO2: Natural variations Archean to present, 32, 99–110, https://doi.org/10.1029/GM032p0099, 1985.
92. Wakeham, S.G., Peterson, M.L., Hedges, J.I. and Lee, C.: Lipid biomarker fluxes in the Arabian Sea, with a comparison to the equatorial Pacific Ocean. Deep Sea Research Part II: Topical Studies in Oceanography, 49, 2265–2301, https://doi.org/10.1016/S0967-0645(02)00037-1, 2002.

https://doi.org/10.5194/egusphere-2024-845
Preprint. Discussion started: 24 April 2024

93. Ward, B.B., Devol, A.H., Rich, J.J., Chang, B.X., Bulow, S.E., Naik, H., Pratihary, A. and Jayakumar, A.: Denitrification as the dominant nitrogen loss process in the Arabian Sea, Nature, 461, 78–81, https://doi.org/10.1038/nature08276, 2009.
94. Wishner, K.F., Gowing, M.M. and Gelfman, C.: Mesozooplankton biomass in the upper 1000 m in the Arabian Sea: overall seasonal and geographic patterns, and relationship to oxygen gradients, Deep Sea Research Part II: Topical Studies in Oceanography, 45, 2405–2432, https://doi.org/10.1016/S0967-0645(98)00078-2, 1998.
95. Wittenborn, A.K., Schmale, O. and Thiel, V.: Zooplankton impact on lipid biomarkers in water column vs. surface sediments of the stratified Eastern Gotland Basin (Central Baltic Sea), Plos one, 15, e0234110, https://doi.org/10.1371/journal.pone.0234110, 2020.
96. Xiong, W., Mei, X., Meng, X., Chen, H. and Yang, H.: Phytoplankton biomarkers in surface sediments from Liaodong Bay and their potential as indicators of primary productivity, Marine Pollution Bulletin, 159, 111536, https://doi.org/10.1016/j.marpolbul.2020.111536, 2020.
97. Zúñiga, D., Sanchez-Vidal, A., Flexas, M.D.M., Carroll, D., Rufino, M.M., Spreen, G., Calafat, A. and Abrantes, F.: Sinking diatom assemblages as a key driver for deep carbon and silicon export in the Scotia Sea (Southern Ocean), Frontiers in Earth Science, 9, 579198, https://doi.org/10.3389/feart.2021.579198, 2021.

https://doi.org/10.5194/egusphere-2024-845
Preprint. Discussion started: 24 April 2024

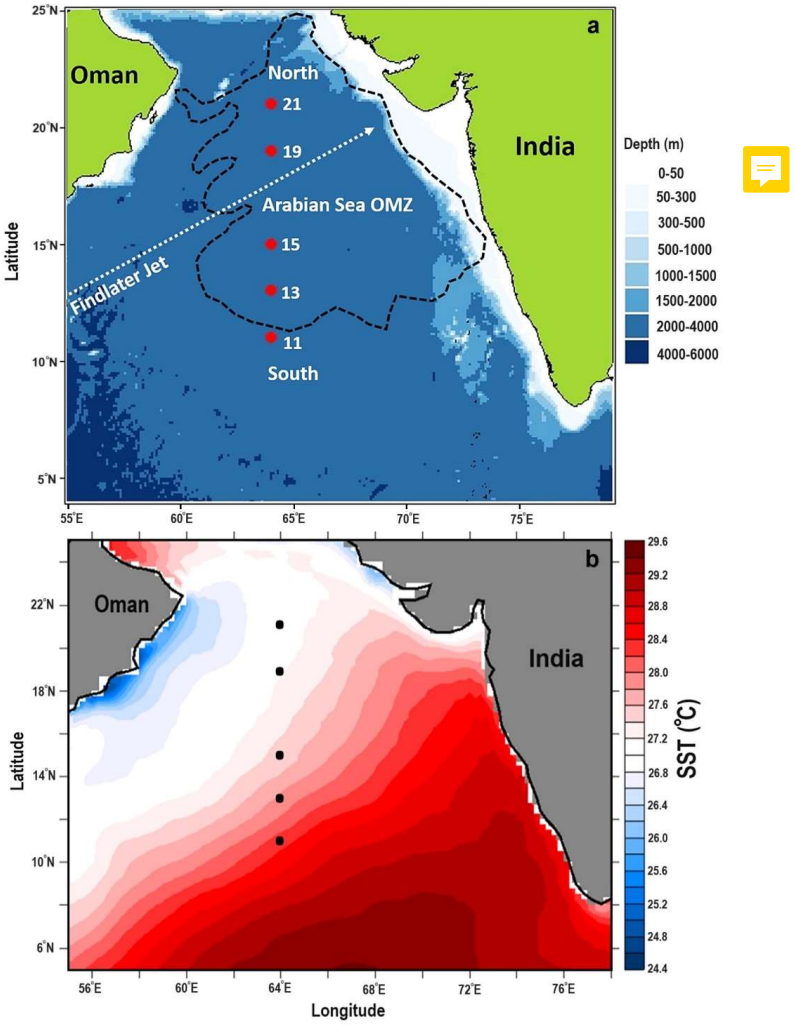

Figure 1. Map showing the study location in the Central Arabian Sea along 64° E transect during SSD-068 (Dec 2019) (a). The low-level atmospheric jet (Findlater Jet) is shown by a white dashed arrow and the boundary of the Oxygen Minimum Zone (OMZ) (0.5 mmol L^{-1} O_2 concentration) is shown by a black dashed line. The average SST (2017-2020) values depicting spatial variability among the sampling stations from the north to south (b).

https://doi.org/10.5194/egusphere-2024-845
Preprint. Discussion started: 24 April 2024

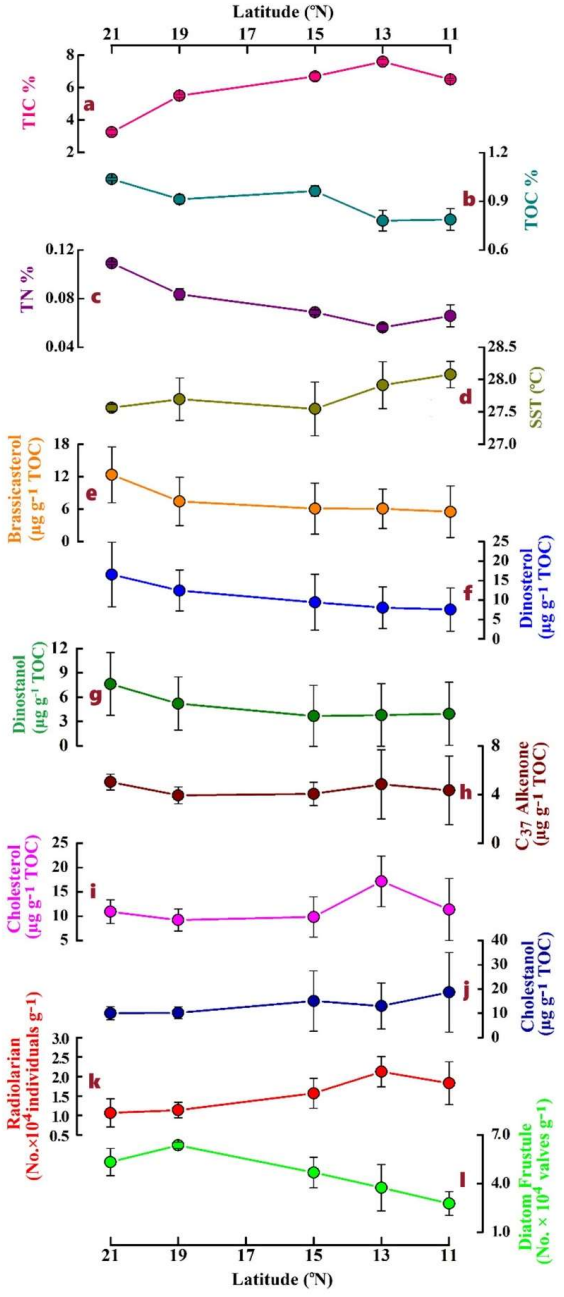

Figure 2. The distribution of total inorganic carbon (TIC %) (a), total organic carbon (TOC %) (b), total nitrogen (TN%) (c), sea surface temperature (SST °C) (d), brassicasterol (e), dinosterol (f), dinostanol (g), C_{37} alkenones (h), cholesterol (i), cholestanol (j), radiolarians (k), and diatom frustules (l) along the 64° E transect in the central Arabian Sea.

https://doi.org/10.5194/egusphere-2024-845
Preprint. Discussion started: 24 April 2024

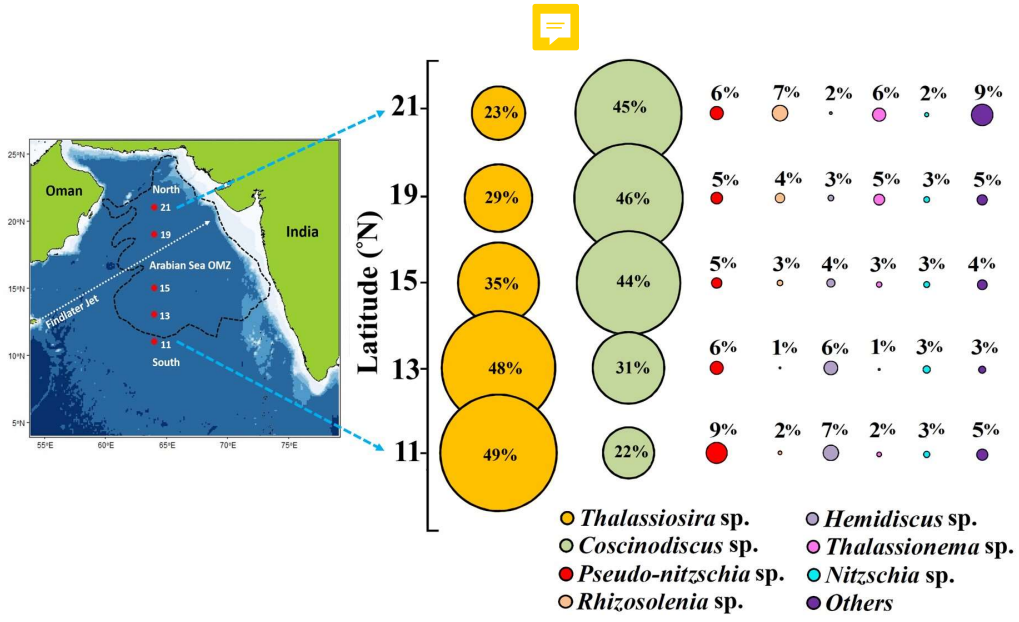

Figure 3. The relative percentage of diatom frustules of major species (>3% of total abundance) from surface sediment samples (top 0.5, 1 cm) along the 64° E transect in the central Arabian Sea. Individual contributions from centric and pennate diatoms <3% were summed as "others".

https://doi.org/10.5194/egusphere-2024-845
Preprint. Discussion started: 24 April 2024

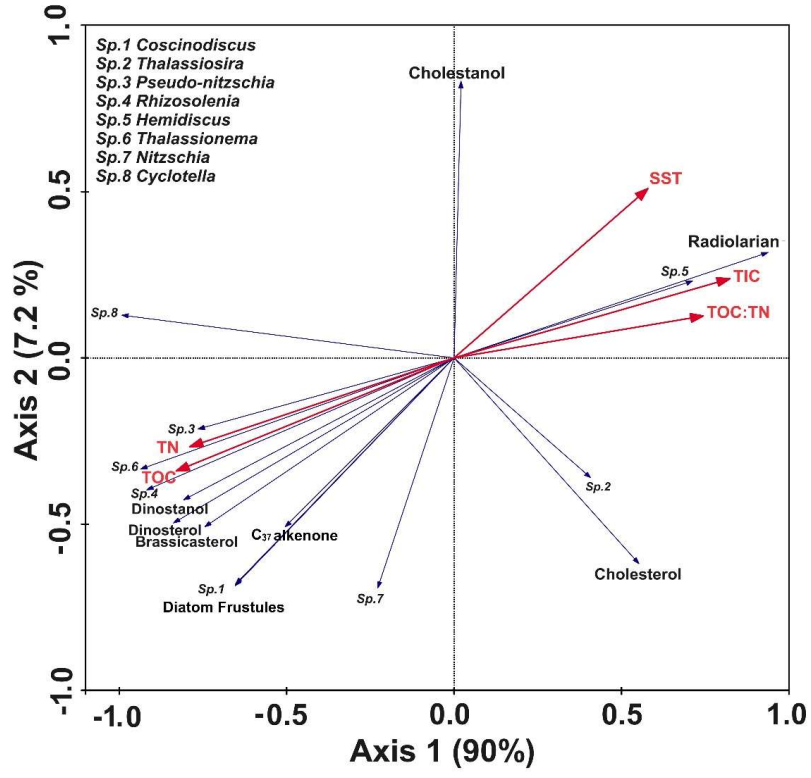

Figure 4. RDA biplot shows the interrelationship between the biotic and abiotic factors. The names of diatoms genera are marked as "Sp." and are mentioned in the top left side of the panel**.** Axis 1 and axis 2 explained nearly 97.2% of variability.

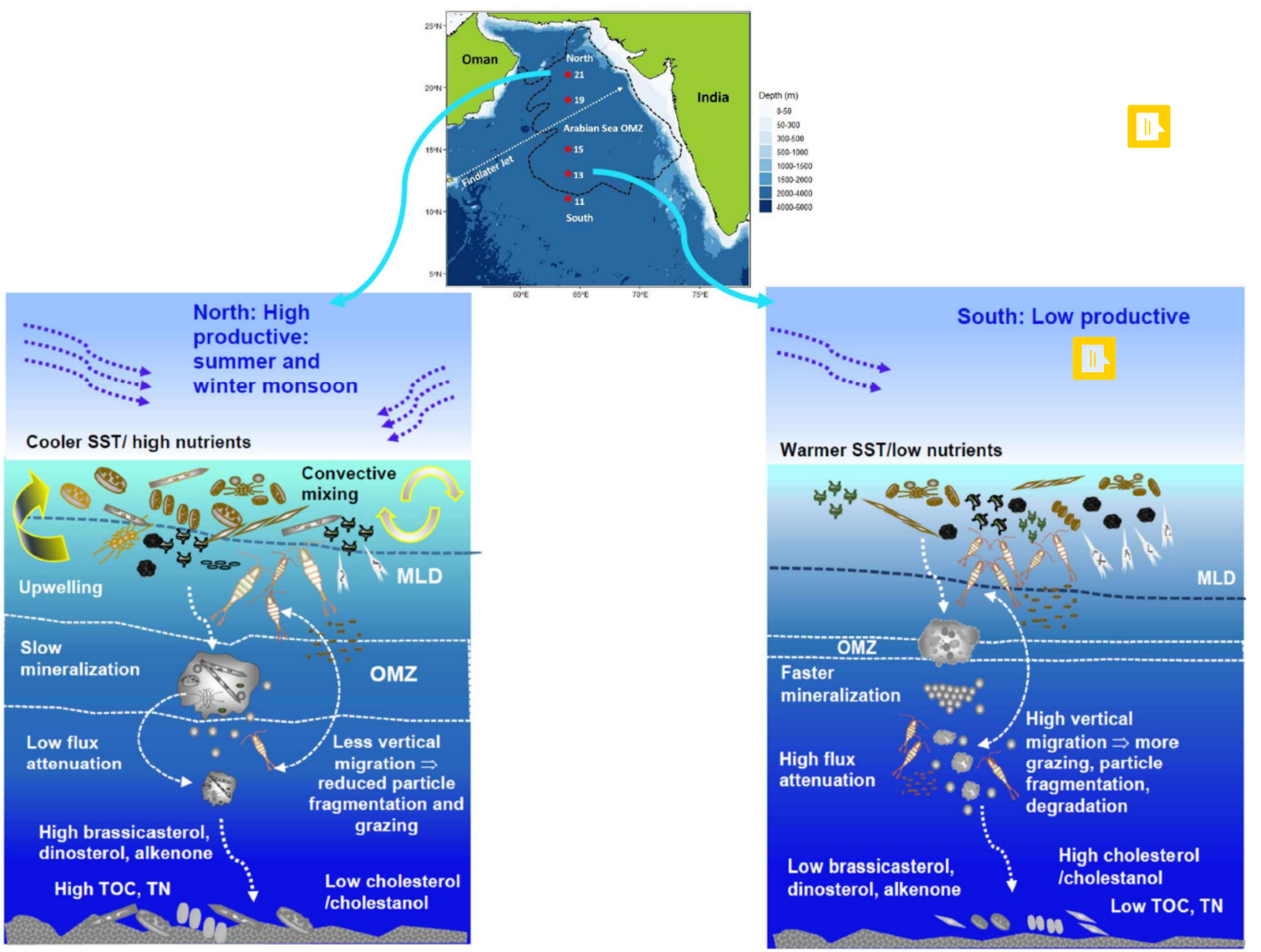

Figure 5. The schematic shows the spatial variability in particle flux along the 64° E transect in the central Arabian Sea.

https://doi.org/10.5194/egusphere-2024-845
Preprint. Discussion started: 24 April 2024

1060 **Table 1.** Sedimentary characteristics, diatom frustules, and sterol concentrations in the surface sediments from the central Arabian Sea
1061 (n =2±SD). The values represent the average from 0.5 and 1 cm core slices.

Latitude (°N)	C %	TOC %	TN %	TOC: TN	Alkenone based SST (°C)	Diatom frustule (No.×10^4 valves g^{-1})	Radiolarian (No.×10^4 individuals g^{-1})	Brassicasterol (ng g^{-1})	Dinosterol (ng g^{-1})	Dinostanol (ng g^{-1})	C_{37} alkenone (ng g^{-1})	Cholesterol (ng g^{-1})	Cholestanol (ng g^{-1})	Dinosterol: Brassicasterol	Brassicasterol:Alkenone
21	3.25±0.15	1.04±0.01	0.11±0.001	9.5±0.18	27.6±0.05	5.33±0.83	1.07±0.36	128.0±52.6	171.1±84.4	79.0±39.4	52.2±6.3	113.2±24.4	104.4±26.9	1.31	2.41
19	5.50±0.09	0.91±0.03	0.08±0.005	10.9±0.28	27.7±0.33	6.36±0.20	1.14±0.20	68.6±43.0	114.2±51.4	48.0±31.5	36.0±7.4	84.4±23.3	93.7±24.6	1.78	1.82
15	6.70±0.24	0.96±0.03	0.07±0.002	14±0.08	27.5±0.42	4.69±0.94	1.57±0.38	58.2±43.5	89.8±66.2	34.7±35.2	39.0±8.0	94.1±36.8	143.5±115.1	1.55	1.41
13	7.60±0.13	0.78±0.06	0.06±0.003	13.9±1.83	27.9±0.36	3.75±1.43	2.13±0.39	46.4±24.4	61.0±36.7	28.3±27.8	36.9±19.1	132.3±29.5	98.6±65.3	1.28	1.25
11	6.51±0.06	0.79±0.07	0.07±0.009	12.1±2.69	28.1±0.20	2.78±0.73	1.83±0.55	42.0±33.9	57.7±38.8	29.8±28.0	33.3±19.3	87.3±42.9	141.6±116.5	1.49	1.16
Average±SD	5.91±1.66	0.90±0.11	0.08±0.02	12.1±1.9	27.8±0.2	4.58±1.39	1.54±0.45	68.62±34.77	98.76±46.53	43.95±21.05	39.47±7.39	102.27±20.21	116.37±24.22	1.5±0.2	1.6±0.5

1062

1063

1064 **Table 2.** Average values of various parameters (n =2, ±SD) from the northern (21, 19, and 15° N) and southern stations (13 and 11° N)
1065 of the central Arabian Sea. The values shown in **bold** "*p*" represent the level of significance (single-factor ANOVA at 95% confidence
1066 level) between the northern and the southern stations.
1067

Parameter	North	South	*p*-value
Total Inorganic Carbon (TIC %)	5.15±1.57	7.06±0.63	**0.05**
Total Organic Carbon (TOC %)	0.97±0.06	0.78±0.05	**0.0009**
Total Nitrogen (TN %)	0.087±0.018	0.061±0.008	**0.03**
Alkenone derived SST (°C)	27.6±0.25	28.0±0.26	**0.043**
Diatom frustules (No.×10^4 valves g^{-1})	5.46±0.95	3.26±1.08	**0.009**
Radiolarian (No.×10^4 individuals g^{-1})	1.26±0.35	1.98±0.43	**0.019**
Brassicasterol (µg g^{-1} TOC)	8.64±4.75	5.81±3.48	0.3
Dinosterol (µg g^{-1} TOC)	12.81±6.30	7.80±4.47	0.2
Dinostanol (µg g^{-1} TOC)	5.50±3.35	3.87±3.17	0.46
C_{37} alkenone (µg g^{-1} TOC)	4.34±0.81	4.60±2.33	0.8
Cholesterol (µg g^{-1} TOC)	9.99±2.50	14.26±5.83	0.14
Cholestanol (µg g^{-1} TOC)	11.80±6.33	15.85±11.39	0.49
Dinosterol: Brassicasterol	1.55±0.27	1.39±0.21	0.34
Brassicasterol: Alkenone	1.88±0.76	1.21±0.21	0.13

1068

https://doi.org/10.5194/egusphere-2024-845
Preprint. Discussion started: 24 April 2024